

# A revision to the background vertical diffusion scheme of Peters *et al.* (1988)

Ocean Applications Technical Note No. 33

S. Cusack

January 2004

Produced by the Met Office

Met Office FitzRoy Road Exeter Devon EX1 3PB United Kingdom

Tel +44 (0)1392 886465 Fax: +44 (0)1392 884499

E-mail: [matthew.martin@metoffice.com](mailto:matthew.martin@metoffice.com) [www.metoffice.com](http://www.metoffice.com)

## 1. Introduction

Figure 1a shows a map of monthly mean SST in the tropical Pacific Ocean for a development version of the Hadley Centre Global Environment Model version 1 (HadGEM1) which is close to the final, frozen version of this climate model. There is a significant amount of noise in the SST field, in the horizontal, and this has been a characteristic of all HadGEM1 development versions. The amplitude of the noise is quite constant throughout the integration. Figure 1b shows a cross-section of potential temperature at the equator in the Pacific Ocean, and illustrates that the noise in the temperature field is three dimensional. The operational climate model that HadGEM1 will replace, the Hadley Centre Coupled Model version 3 (HadCM3) has similar noise characteristics in this region, though of lesser magnitude than in HadGEM1.

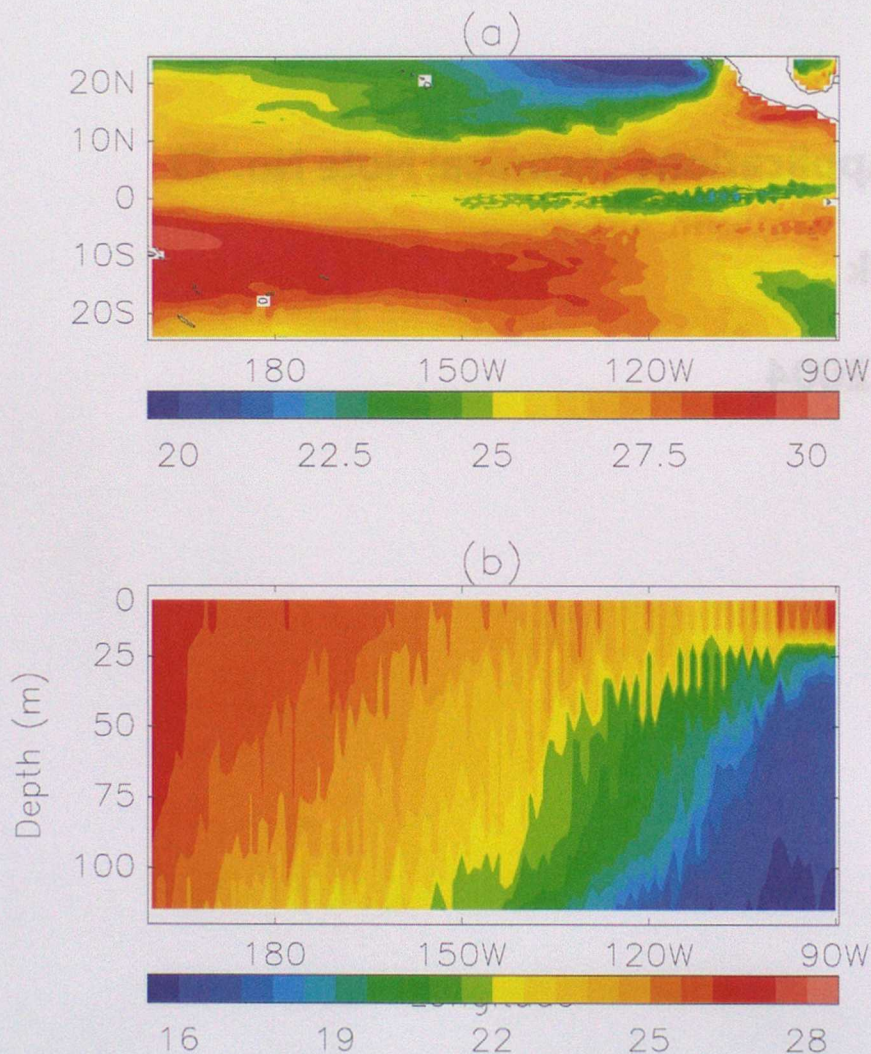


Figure 1: (a) map of monthly mean SST for Feb 1979 for a near-final HadGEM1 development run, (b) the corresponding cross-section at the equator.

This report shows results from a diagnostic study designed to identify the model parametrization which is the source of this noise in Section 2, and in Section 3 this noise source is critically reviewed, and it is found to be due to a parametrization method which is inappropriate for a large-scale model. Results from HadGEM1 tests

of a more accurate method of parametrizing the process are presented in Section 4. A summary of this work is given in Section 5.

## 2. The cause of the noise in ocean temperature fields

A heat budget analysis on a timestep-by-timestep basis was performed on a short HadGEM1 integration, and Figure 2 shows results at the time when significant spatial noise first appears for the total temperature increment in a timestep. At about 115W, the total theta increment in the timestep is noisy in the horizontal direction in the top two layers (Figure 2a). The major contributor to this noise is the temperature increments from the vertical diffusion process (Figure 2b).

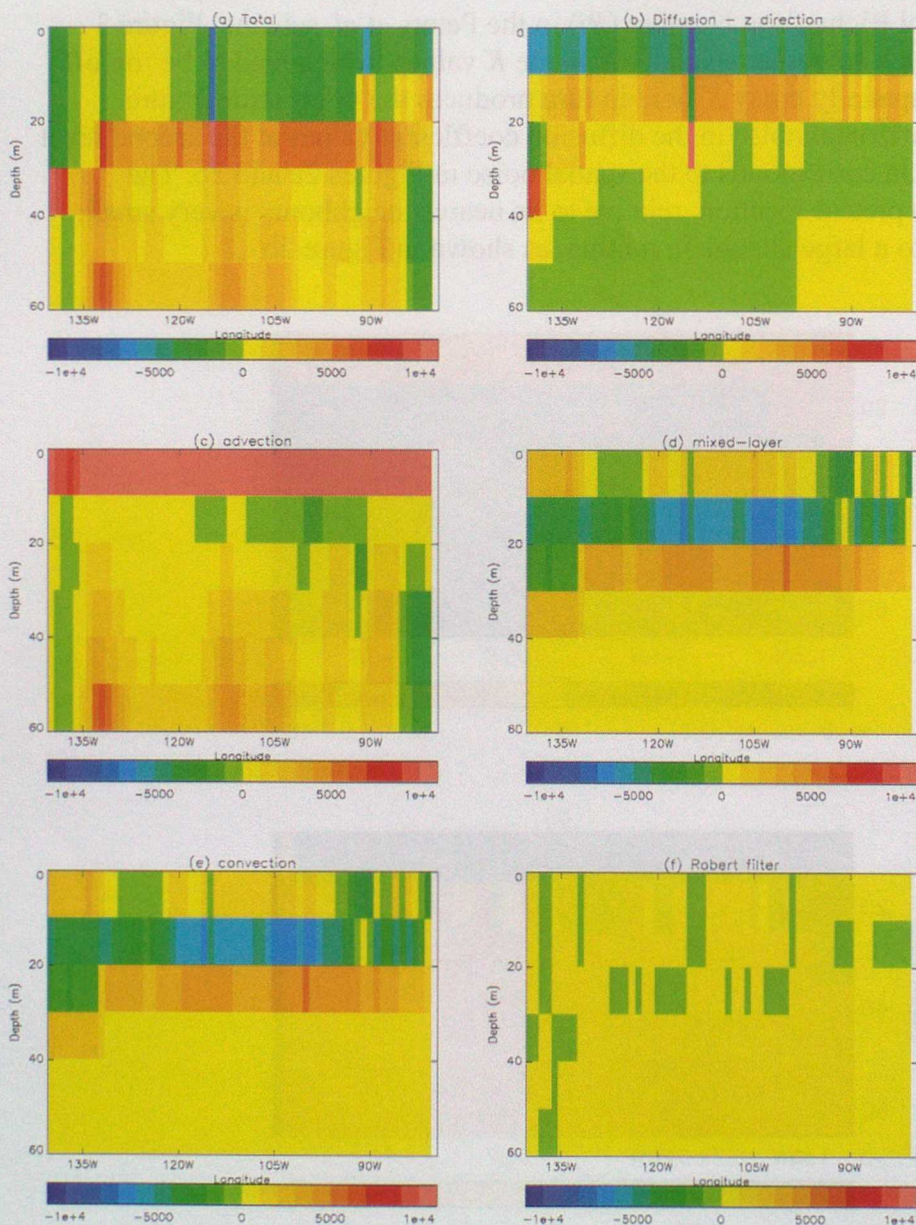


Figure 2: equatorial Pacific Ocean cross-section of the change of theta at timestep 23: (a) the total change, (b) diffusion in the z direction, (c) advection, (d) mixed-layer scheme, (e) convection and (f) Robert filter.

The vertical diffusion scheme is hybrid in nature, composed of a background vertical mixing scheme, based on Peters *et al.* (1988), together with a scheme for more rapid mixing of tracers at the surface, the Kraus-Turner scheme (see Foreman, 1990), and mixing of momentum at the surface, which uses a simplified version of the Large *et al.* (1994) scheme. All these schemes are documented in Rickard, 1999. To isolate which vertical mixing scheme was responsible for the noise, a test was set-up which modified the Peters *et al.* scheme to output spatially uniform mixing coefficients. This test produced no spatial noise in the temperature field, thereby indicating that the Peters *et al.* scheme is responsible for the noise in HadGEM1.

The Peters *et al.* scheme has a simple formulation. The increment from this scheme is found by solving the standard diffusion equation, which in turn requires an estimate of the local diffusion coefficient ( $K$ ) between two levels.  $K$  is specified solely as a function of the local Richardson Number ( $Ri$ ) in the Peters *et al.* scheme. Figure 3 shows that  $Ri$  is much smoother spatially than the  $K$  values, which tend to be 'on/off' in behaviour. The spatially noisy  $K$  field in turn produces the noisy temperature increments. The horizontal noise in the diffusion coefficient values at the second level at 115W in Figure 3a corresponds to the spatial noise in Figures 2a and 2b. The change in  $Ri$  at this precise location, relative to its nearest neighbours is very small, yet it corresponds to a large change in mixing, as shown in Figure 2b.

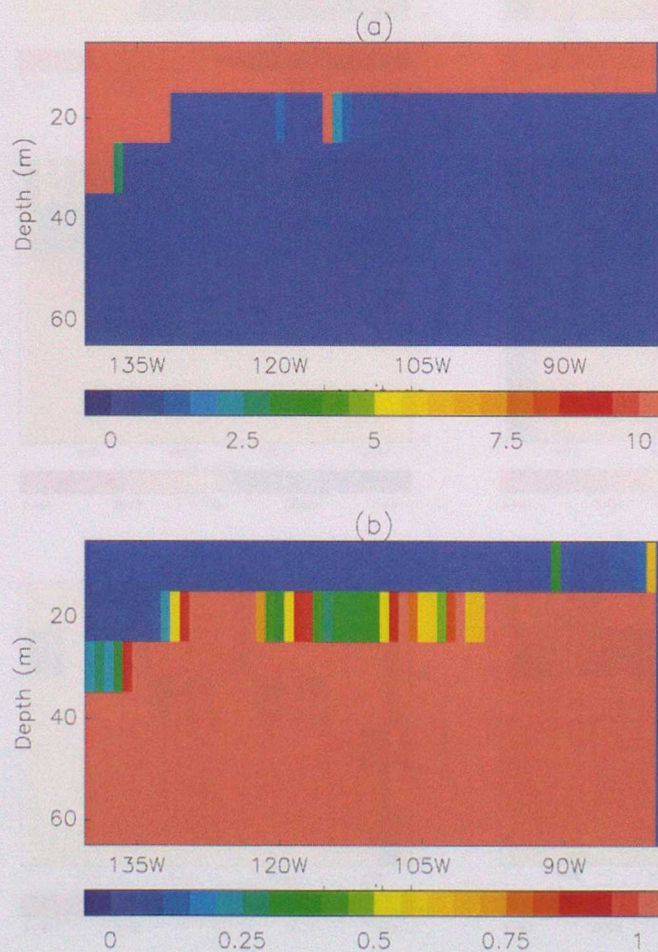


Figure 3: a cross-section in the equatorial Pacific Ocean at timestep 23 of (a) the diffusion coefficient for tracers, and (b) the Richardson Number for tracers.

### 3. A critical review of the Peters *et al.* scheme

Figure 3 shows that a spatially smooth input field can be transformed into a noisy output field from the Peters *et al.* scheme. This is due to the functional form relating the diffusion coefficient ( $K$ ) to the gradient Richardson Number ( $Ri$ ), see equations (10) to (13) of Peters *et al.* (1988). At low values of  $Ri$  the  $K$  values for heat diffusion are proportional to  $Ri^{-9.6}$ , causing very large increases in  $K$  for very small changes in  $Ri$ . This very large exponent is the cause of the noise in the ocean potential temperature fields in HadGEM1.

It was mentioned in the first section that HadCM3 has noise in the equatorial Pacific Ocean, of a smaller amplitude than in HadGEM1. This could be due to the use of the Pacanowski and Philander (1981) scheme in HadCM3 rather than the Peters *et al.* scheme: the former has a parametrized dependence of  $K$  on  $Ri$  with an exponent of -3, so the magnitude of the rate of change of  $K$  with respect to  $Ri$  is less with Pacanowski and Philander, thus one would expect less noise. A short HadGEM1 test was performed using the Pacanowski and Philander formulation in place of the Peters *et al.* scheme, and the noise amplitude was smaller in the tropical Pacific Ocean.

The parametrization method of Peters *et al.* (1988) used to determine  $K$  as a function of  $Ri$  is now examined. Observations of quantities such as the profile of temperature and currents, and the amount of vertical mixing, were made at 20 min intervals, then the data were averaged to form hourly mean values. Peters *et al.* chose to average these data over a 4.5 day period, then to calculate the mean  $K$  and  $Ri$  values at different depths from these averaged values, before implementing a standard curve-fitting method to determine  $K$  as a function of  $Ri$ . Their decision to average the data over a 4.5 day period was made in order to "average over the diurnal cycle and over higher-frequency variations which are commonly not represented explicitly in numerical models".

The timestep of the ocean model is one hour, therefore a parametrization built on 4.5 day average values has an inappropriate timescale. Furthermore, the ocean model effectively treats quantities as instantaneous values, and the effect of the finite model timestep, often referred to as truncation error, is a separate issue which cannot be properly treated by pre-processing the data before the curve-fitting procedure is applied.

The pre-processing of observed data by Peters *et al.* was examined further. In all the fits reported below, the curve-fitting methodology was identical, and is described in the Appendix. Briefly, the following functional form was assumed for the relationship between  $K$  and  $Ri$ :

$$K = ARi^b + CRi^d \quad (1)$$

Hartmut Peters supplied the hourly averaged observations of the basic variables, and different averaging timescales were applied to these data and the resulting fit coefficients are displayed in Table 1. Trends can be seen in different coefficients: in particular, note that the exponent  $b$  is of smaller magnitude as the averaging timescale

is reduced. It is this coefficient which determines the steepness of the  $K$  versus  $Ri$  slope at low  $Ri$ .

**Table 1** – the coefficients for the fit between  $K$  and  $Ri$  for different timescales over which  $K$  and  $Ri$  are averaged.

	4 days	2 days	12 hours	3 hours	1 hour
A	$2.5 \times 10^{-5}$	$7.6 \times 10^{-4}$	$1.6 \times 10^{-3}$	$3.6 \times 10^{-3}$	$3.4 \times 10^{-3}$
b	-9.49	-6.27	-5.62	-4.33	-3.89
C	0.065	0.039	0.017	0.010	$9.4 \times 10^{-3}$
d	-0.53	-0.5	-0.26	-0.20	-0.28

The instantaneous data upon which the hourly averages were based were recorded every 20 mins, and such data is not available at present. The patterns evident in Table 1 indicate that the use of instantaneous data every 20 min may produce a similar  $b$  coefficient to that obtained when using the hourly averaged data.

If one believes a relationship exists between two observed variables,  $X$  and  $Y$ , then one cannot apply an operator and effectively transform the data to  $X'$  and  $Y'$ , before looking for the relationship between these variables. In general, a different operator would lead to a different behaviour between the two variables, as can be seen in Table 1, and this is undesirable. Peters *et al.* (1988) applied a time-averaging operator to their observations before doing the curve-fitting procedure, so as to remove high frequency variations with a timescale less than 4.5 days. It is recommended that such pre-processing of data is abandoned, and that the data with the smallest averaging timescale be used. This will also lead to a less steep gradient of  $K$  versus  $Ri$ , and therefore to a smaller amplitude of noise in ocean temperature fields.

#### 4. Results from a HadGEM1 test of the revised Peters *et al.* scheme

A modification was made to a version of HadGEM1 which was close to the final, frozen version. This modification replaced the Peters *et al.* (1988) parametrization of ocean vertical diffusion of momentum and tracers with that represented by equation (1), using the coefficients in the last column of Table 1. In effect, the curve-fitting procedure has been applied to data which has been averaged over a one hour rather than a 4.5 day timescale. This test was integrated for 10 years and 9 months. Figure 4 shows the time series of Nino3 SST values for this test and its control. An analysis of the impact of this change on ENSO (Buwon Dong, personal communication) concludes that no clear ENSO signal can be found, for a test of this duration. The reduced magnitude of the  $b$  parameter in this test reduces the noise in the ocean temperature fields, which was the motivation for this work, although there seems to be no other significant signal in the ocean model's behaviour. An assessment of the changes to the atmosphere simulation concluded that the test signal was not significantly different from the natural variability of the control run.

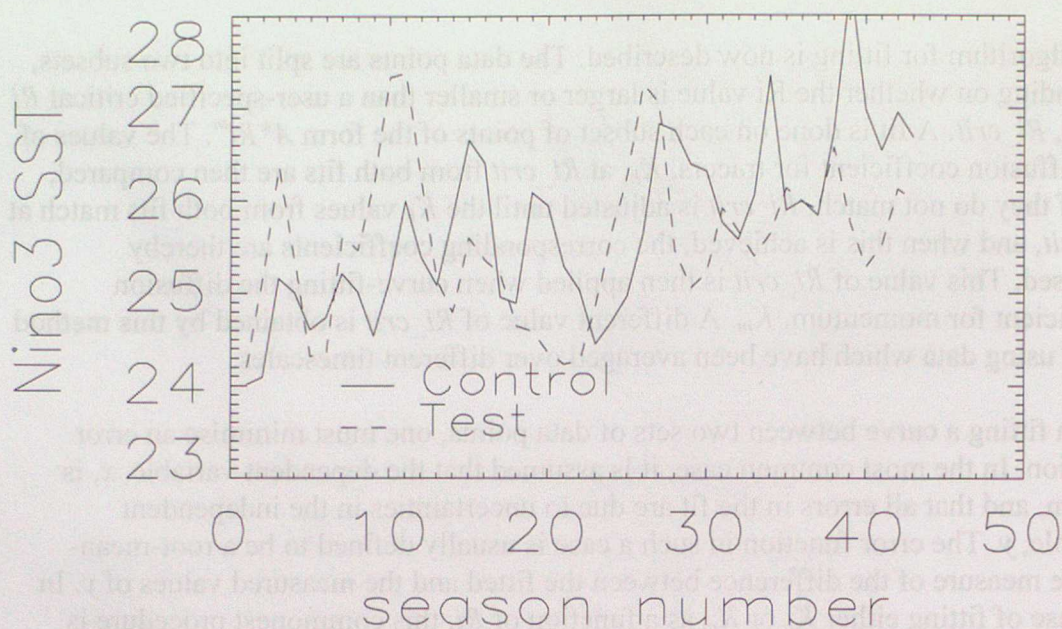


Figure 4: a time series of the SST averaged over the Niño3 region for a control (a near-final version of HadGEM) and a test using the Peters *et al.* functional form with hourly averaged data.

## 5. Summary

The cause of the spatial noise in the temperature fields in the eastern tropical Pacific Ocean in HadGEM1 is the Peters *et al.* (1988) scheme for background vertical diffusion. The Peters *et al.* scheme calculates increments to fields by solving the standard diffusion equation, and using an estimate of the  $K$  value based solely on  $Ri$ . The  $K$  values can be extremely sensitive to  $Ri$  at low values of  $Ri$ , where the functional form  $K \propto Ri^{-9.6}$  is used. Spatially smooth input fields can cause noisy increments to temperature and salinity because of this behaviour of  $K$  at low  $Ri$ .

An investigation of the method used by Peters *et al.* to calibrate the relationship between  $K$  and  $Ri$  revealed that the averaging of these variables over 4.5 day periods led to a best-fitting exponent with a magnitude of 9.6. If one uses a more appropriate averaging period of one hour, the best-fitting relationship between  $K$  and  $Ri$  at low  $Ri$  has an exponent of magnitude 4.0. This leads to less noisy temperature increments being generated by the background vertical diffusion scheme in HadGEM1. In a 13 year test, there is no discernible signal in ENSO patterns with this revised Peters *et al.* scheme, and no significant signals in the atmosphere component of HadGEM1.

## Appendix - The curve-fitting method

The algorithm for fitting is now described. The data points are split into two subsets, depending on whether the  $Ri$  value is larger or smaller than a user-specified critical  $Ri$  value,  $Ri_{crit}$ . A fit is done on each subset of points of the form  $A * Ri^m$ . The values of the diffusion coefficient for tracers,  $K_h$ , at  $Ri_{crit}$  from both fits are then compared, and if they do not match,  $Ri_{crit}$  is adjusted until the  $K_h$  values from both fits match at  $Ri_{crit}$ , and when this is achieved, the corresponding coefficients are thereby finalised. This value of  $Ri_{crit}$  is then applied when curve-fitting the diffusion coefficient for momentum,  $K_m$ . A different value of  $Ri_{crit}$  is obtained by this method when using data which have been averaged over different timescales.

When fitting a curve between two sets of data points, one must minimise an error function. In the most common case, it is assumed that the dependent variable,  $x$ , is known, and that all errors in the fit are due to uncertainties in the independent variable,  $y$ . The error function in such a case is usually defined to be a root-mean-square measure of the difference between the fitted and the measured values of  $y$ . In the case of fitting either  $K_h$  or  $K_m$  as a function of  $Ri$ , this commonest procedure is appropriate, for reasons which are now given.

Peters *et al.* (1988) define  $K_m = \epsilon / \text{shear}^2$ , and  $K_h = \chi / (\partial T / \partial z)^2$  ( $\epsilon$  is the rate of viscous dissipation of turbulent kinetic energy, and  $\chi$  is the rate of diffusive smoothing of turbulent temperature fluctuations). The errors quoted in the last paragraph of section 2 of this paper state that hourly averaged shear values have 95% confidence limits of  $0.001 \text{ sec}^{-1}$ . The data at low  $Ri$ , which we are most interested in, are from high shear regions, and errors are less than 10%. The errors in  $\epsilon$  are quoted as a factor of about two, and those for  $\chi$  are about a factor of three (third and second last paragraphs in section 2 respectively). Therefore, errors in  $K_h$  and  $K_m$  are dominated by errors in  $\epsilon$  and  $\chi$ , respectively. Also note that these dominant errors are quoted as factors, therefore the use of error estimates in log space for  $K_h$  and  $K_m$  would seem to be appropriate.  $Ri = N^2 / \text{shear}^2$ , where  $N^2$  is a measure of the gradient of density. There is no reference to errors in  $N^2$  in Peters *et al.* (1988), implying that such errors are relatively small (several pages are devoted to quantifying errors in  $\epsilon$  and  $\chi$  in the Appendix). Therefore, fitting a line by minimising the errors in the fitted  $K$  values in log space is a satisfactory approximation given the nature of the errors in the observations.

## Acknowledgements

Thanks to Hartmut Peters for supplying the data upon which the results in Table 1 are based, and to Helene Banks for help in producing this Technical Note.

## References

Foreman, S.J., 1990: Ocean Model Mixed Layer Formulation. *Unified Model Documentation Paper No.41*.

Large, W.G., J.C.McWilliams and S.C.Doney, 1994: Oceanic vertical mixing: A review and a model with nonlocal boundary layer parameterisation, *Revs. Of Geophys*, **32**, 363-403

Pacanowski, R.C. and S.G.H. Philander, 1981: Parameterization of Vertical Mixing in Numerical Models of Tropical Oceans. *Journal of Physical Oceanography*, **11**, 1443-1451

Peters, H., M. C. Gregg and J. M. Toole, 1988: On the Parameterization of Equatorial Turbulence. *J. Geophys. Res.*, **93**, 1199-1218

Rickard, G., 1999: Ocean Models and the Implementation of Vertical Diffusion and Vertical Mixing. *Unified Model Documentation Paper No.59*.